Chapter 1
Sequential Monte Carlo Methods for Localisation in Wireless Networks

Lyudmila Mihaylova*, Donka Angelova** and Anna Zvikhachevskaya*

Abstract – Wireless indoor and outdoor localisation systems received a great deal of attention in recent years. This chapter surveys first the current state-of-the-art of localisation techniques. Next, it formulates the problem of localisation within Bayesian framework and presents sequential Monte Carlo methods for localisation based on received signal strength indicators (RSSIs). Multiple model particle filters are developed and their performance is evaluated based on RSSIs by accounting for and without considering the measurement noise time correlation. A Gibbs sampling algorithm is presented for estimating the unknown parameters of the measurement noise which highly increases the accuracy of the localisation process. Two approaches to deal with the correlated measurement noises are proposed in the framework of auxiliary particle filtering: with a noise augmented state vector and the second approach implements noise decorrelation. The performance of the two proposed multi-model auxiliary particle filters (MM AUX-PFs) is validated over simulated and real RSSIs and high localisation accuracy is demonstrated.

Key words: sequential Monte Carlo methods, auxiliary particle filtering, localisation, wireless networks, correlated measurement noises, multiple model estimation, parameter estimation, Gibbs sampling

1.1 Motivation

In many every day applications there is a need of finding the position of a moving staff of mobile transportation systems or a vehicle and to know the coordinates

*Lyudmila Mihaylova and Anna Zvikhachevskaya are with the School of Computing and Communications, Lancaster University, InfoLab21, South Drive, Lancaster LA1 4WA, United Kingdom, e-mail: *mila.mihaylova@lancaster.ac.uk, a.zvikhachevskaya@lancaster.ac.uk*,
**Donka Angelova is with the Institute of Information and Communication Technologies, Bulgarian Academy of Sciences, Sofia, Bulgaria, e-mail: *donka@bas.bg*

within a certain geographical region. Other motivating applications include monitoring of large geographical areas, such as for wildlife tracking [1], monitoring of buildings, production processes, warehouses [2] and E-Health systems.

In wireless networks if direct physical connections exist between the mobile unit and the base stations, the channels are considered to be in line-of-sight (LOS) and accurate location estimates can be obtained. However, in urban or indoor environments, the attenuation of the signals is high. Obstacles such as buildings, trees and walls cause obscurations. Reflections and diffractions occur due to shadowing and all these effects cause non-line-of-sight (NLOS). Hence, the movement patterns of mobile users vary significantly in different environments and the location systems should be able to cope with various challenges, such as NLOS, a changeable infrastructure of the wireless network and robustness to sensor failures. It is essential when nodes perform jointly certain tasks, such as decision making, sensor data fusion, object tracking [3–7] to localise the node positions and movement [2, 8, 9], as the transmitter range is generally fairly small with respect to the size of the area. Apart from the changeable network topology, the need of communications between the nodes under limited resources (energy, bandwidth), the need of processing noisy data and of overcoming losses pose additional challenges.

1.1.1 Methods for Localisation

There is a great deal of methods for localisation (see, e.g., the surveys [2, 8, 10–12]) between which the *range-based* [2,13,14] methods are widely used. They rely on the distances between nodes and are usually evaluated using received signal strengths, signal time-of-arrivals, time difference of arrivals or angle-of-arrivals and they vary in their complexity and accuracy. The range-based techniques can be divided into *radio frequency* (RF) ranging and *acoustic ranging*. The radio frequency ranging relies on the premise that by measuring the received signal strength a receiver can determine its distance to a transmitter. Another class of ranging schemes measures the time difference of arrival of acoustic and ultrasonic signals [13, 15].

While range-based algorithms need point-to-point distance estimation or angle estimation for positioning, *range-free* [16] algorithms do not require this information. Another classification subdivides the approaches for mobile nodes localisation in wireless networks to approaches for *indoor* and *outdoor* environment [12]. In [17–19] indoor localisation sensing systems are surveyed. Recently, another approach for indoor localisation has been proposed, called *fingerprinting localisation* [20, 21] which uses power maps, usually created offline. The main idea is to match the observed RSSIs with the map of previously measured RSSIs. Outdoor, Global Positioning Systems (GPSs) and differential GPSs [22] are the most successful systems.

From the point of view of the methods employed, a number of localisation techniques rely on Extended Kalman filters [23, 24], Hidden Markov models [25, 26] (for coping with NLOS), Monte Carlo methods [10, 27–29], including nonparamet-

ric belief propagation [30], and on the knowledge of the connectivity between the nodes. Communications between nodes during the localisation process are reduced to minimum due to energy and bandwidth constraints.

In [31] and [32] multiple model particle filtering techniques for mobility tracking of users in cellular networks are developed. A particle filter, a Rao-Blackwellised particle filter are presented and their performance is compared with an Extended Kalman filter over simulated and real data from base stations. In [33,34] an auxiliary multiple model particle filter (PF) is proposed for bearings-only tracking problems. In [33] a deterministic splitting of each particle into several offsprings is performed for manoeuvring target tracking, each offspring representing a different target manoeuver. In [35] an auxiliary PF is designed for target tracking in binary sensor networks. When the measurements are co-linear a simulated annealing approach, such as the proposed in [36] can cope with these ambiguities.

Most of the above mentioned works, however, do not take into account the correlation of the measurement noise which can deteriorate significantly the localisation accuracy. One of the most common correlation models for the slow shadow fading component is proposed by Gudmunsson [37]. The model of Gudmunsson consists of a decreasing autocorrelation function. The same first-order autoregressive correlation model is used in [38], jointly with a Kalman filter aimed to estimate the correlation coefficient of the shadowing component of the measurements. The shadow fading correlation properties are studied also in [39].

In our work we propose a solution to the self-localisation problem of mobile nodes by taking into account the temporal correlation in the measurement noise. The methods that we present are general, although the applications considered are for outdoor localisation. They can be applied also in indoor environment if a map is available. This chapter generalises several sequential Monte Carlo techniques based on [28,31,32,40,41]. Multiple model auxiliary particle filtering techniques are proposed for localisation of a single or several mobile nodes in wireless sensor networks. Their performance is validated on simulated and real RSSIs, over scenarios with several nodes and with a single mobile node, respectively. Similarly to [37], the correlated noise is modeled by a first order autoregressive model. Two approaches that can deal with the correlated measurement noises are described. The first one augments the state vector with the measurement noise, the second approach implements a noise decorrelation by introducing the so called "differenced measurement" [42]. The two approaches for localisation under measurement noise uncertainty are implemented in the multiple model auxiliary particle filter framework and their performance is validated.

In the considered formulation of the problem, node mobility is modeled as a linear system driven by a discrete-time command Markov process whereas the measurement models are nonlinear and necessitate a reliable nonlinear estimation method. Due to the fact that the control process of the mobile nodes is unknown, node mobility is modeled with multiple acceleration modes (regimes). The proposed nonlinear estimation techniques can incorporate physical constraints and possibly communications among frequently manoeuvring mobile nodes in the form of additional measurements.

The remaining part of the chapter is organised as follows. Section 1.2 formulates the considered problem for localisation of mobile nodes and describes the motion model and the observation model. A multiple model auxiliary particle filter for mobile nodes self-localisation is described in Section 1.3. The unknown measurement noise parameters can be estimated with a Gibbs sampling algorithm presented in Sections 1.4 and 1.5. Performance evaluation of the proposed Gibbs sammpling combined with the multiple model auxiliary particle filter is performed in Sections 1.6 and 1.7, over simulated and real data. Finally, Section 1.8 discusses the results and outlines open issues for future research.

1.2 Localisation of Mobile Nodes

Consider the two-dimensional problem of simultaneous localisation of n mobile nodes as formulated in [2]. The vector $\{(x_1,y_1),(x_2,y_2),\ldots,(x_n,y_n)\}$ of positions of the mobile nodes is estimated given n_r reference (anchor) nodes with known coordinates $\{(x_{n+1},y_{n+1}),(x_{n+2},y_{n+2}),\ldots,(x_{n+n_r},y_{n+n_r})\}$ and pairwise measurements $\{z_{ij}\}$, where z_{ij} is a measurement between devices i and j. The reference nodes can obtain their coordinates in the network (through some external means such as a GPS). Apart from their positions, the mobile nodes estimate their speeds and accelerations. This includes applications in which each sensor is equipped with a wireless transceiver and the distance between sensor locations is estimated by RSSI measurements or time delay of arrivals between sensor locations.

1.2.1 Motion Model of the Mobile Nodes

Different mobility models have been developed for localisation in wireless networks, such as random walk and pursue mobility models [43] and Singer-type models [8, 44–46]. Many of the models suggested in the target tracking literature [8, 47, 48] are also applicable for mobile nodes localisation. In this work we adopt the discrete-time Singer-type model [49] because it characterises the correlated accelerations of the mobile as a time correlated process and allows for accurate prediction of the position, speed and acceleration of mobile nodes. This higher-order model affords decreasing the estimation error [8], although mobility models that do not comprise the acceleration can be used too.

The state of each moving node at time instant k is defined by the vector $\boldsymbol{x}_k = (x_k,\dot{x}_k,\ddot{x}_k,y_k,\dot{y}_k,\ddot{y}_k)'$ where x_k and y_k specify the position, $\dot{x}_k$ and $\dot{y}_k$ specify the speed, $\ddot{x}_k$ and $\ddot{y}_k$ are, respectively, the acceleration in x and y directions in the two-dimensional plane; $'$ denotes the transpose operation. The motion of each mobile node can be described by the following Singer model [49, 50]

$$\boldsymbol{x}_k = \boldsymbol{A}(T,\alpha)\boldsymbol{x}_{k-1} + \boldsymbol{B}_u(T)\boldsymbol{u}_k + \boldsymbol{B}_w(T)\boldsymbol{w}_k, \tag{1.1}$$

where $\boldsymbol{u}_k = (u_{x,k}, u_{y,k})'$ is a discrete-time command process, and the respective matrices from (1.1) are in the form

$$\boldsymbol{A}(T,\alpha) = \begin{pmatrix} \tilde{\boldsymbol{A}} & \boldsymbol{0}_{3\times 3} \\ \boldsymbol{0}_{3\times 3} & \tilde{\boldsymbol{A}} \end{pmatrix}, \boldsymbol{B}_i(T) = \begin{pmatrix} \tilde{\boldsymbol{B}}_i & \boldsymbol{0}_{3\times 1} \\ \boldsymbol{0}_{3\times 1} & \tilde{\boldsymbol{B}}_i \end{pmatrix}, \tag{1.2}$$

$$\tilde{\boldsymbol{A}} = \begin{pmatrix} 1 & T & T^2/2 \\ 0 & 1 & T \\ 0 & 0 & \alpha \end{pmatrix}, \tilde{\boldsymbol{B}}_u = \begin{pmatrix} T^2/2 \\ T \\ 0 \end{pmatrix}, \tilde{\boldsymbol{B}}_w = \begin{pmatrix} T^2/2 \\ T \\ 1 \end{pmatrix}. \tag{1.3}$$

The subscript i in the matrix $\boldsymbol{B}(T)$ in (1.2) stands for u or w, respectively. The random process $\boldsymbol{w}_k$ is a 2×1 vector and T is the discretisation period. The parameter α is the reciprocal of the manoeuvre time constant and thus depends on how long the manoeuvre lasts. The process noise $\boldsymbol{w}_k$ is a white sequence, with covariance matrix $E[\boldsymbol{w}\boldsymbol{w}'] = \boldsymbol{Q} = \sigma_w^2 \boldsymbol{I}$, where $E[.]$ is the mathematical expectation operation, $\boldsymbol{I}$ denotes the unit matrix and σ_w is the standard deviation.

The unknown command processes $u_{x,k}$ and $u_{y,k}$ take values from a set of acceleration levels $\mathscr{M}_x$ and $\mathscr{M}_y$. The process $\boldsymbol{u}_k$ takes values from the set

$$\mathrm{M} = \mathscr{M}_\mathrm{x} \times \mathscr{M}_\mathrm{y} \triangleq \{\boldsymbol{u}_1, \ldots, \boldsymbol{u}_\mathrm{r}\}. \tag{1.4}$$

Let $\mathbb{S} \triangleq \{1,2,\ldots,r\}$ denote the set of models and let $m_k \in \mathbb{S}$ be the regime variable, modelled as a first-order Markov chain with transition probabilities $\Pi_{ij} = P(m_k = j | m_{k-1} = i)$, $i,j = 1,\ldots,r$ and initial probability distribution $\tilde{\mu}_{i,0} = P_0\{m = m_i\}$ for $m_i \in \mathbb{S}$ such that $\tilde{\mu}_{i,0} \geq 0$ and $\sum_{i=1}^{r} \tilde{\mu}_{i,0} = 1$.

The next section describes the observation model used in the sequential Monte Carlo methods for localisation.

1.2.2 Observation Model

In wireless networks, the distance between mobile and reference (anchor) nodes can be inferred from RSSIs or pilot signals of nodes. The RSSI $z_{\ell j,k}$ received at the mobile node N_ℓ with coordinates $(x_{\ell,k}, y_{\ell,k})$ at time k, after being transmitted from the node N_j with coordinates $(x_{j,k}, y_{j,k})$, propagates as follows [8, 37, 51]

$$z_{\ell j,k} = \kappa_j - 10\gamma \log_{10}(d_{\ell j,k}) + v_{\ell j,k}, \tag{1.5}$$

where κ_j is a constant depending on the transmission power, wavelength, and gain of node N_j, γ is the slope index (according to [37] $\gamma = 3.3$ for suburban environment and $\gamma = 5$ for microcells in urban environment), $v_{\ell j,k}$ is the logarithm of the shadowing component, which is usually correlated in time, and $d_{\ell j,k}$ is the distance between nodes N_ℓ and N_j

$$d_{\ell j,k} = \sqrt{(x_{\ell,k} - x_{j,k})^2 + (y_{\ell,k} - y_{j,k})^2}. \tag{1.6}$$

All mobile nodes in the group send their pilot signals to the reference nodes. In order to locate a single mobile node in the two-dimensional plane, the three largest RSSIs to reference neighbouring nodes are necessary to enable triangulation. The measurement equation can be written in the form

$$\boldsymbol{z}_k \triangleq (z_{\ell 1,k}, z_{\ell 2,k}, z_{\ell 3,k})' = \boldsymbol{h}(\boldsymbol{x}_k) + \boldsymbol{v}_k, \tag{1.7}$$

where $\boldsymbol{h}(\boldsymbol{x}_k) = (h_{\ell 1,k}, h_{\ell 2,k}, h_{\ell 3,k})'$, is a nonlinear function, with components $h_{\ell j,k} = \kappa_j - 10\gamma \log_{10}(d_{\ell j,k}), j = 1,2,3$, $\boldsymbol{z}_k \in \mathbb{R}^{n_z}$ and $n_z = 3$. The noise $\boldsymbol{v}_k = (v_{1,k}, v_{2,k}, v_{3,k})'$, $\boldsymbol{v}_k \in \mathbb{R}^{n_z}$ with covariance $E[\boldsymbol{v}_k \boldsymbol{v}_k^{'}] = \boldsymbol{R}_k$, characterises the shadowing component.

In the general case with $\ell = 1, \ldots n$ mobile nodes and $j = 1, \ldots n_r$ reference nodes, the overall observation vector will contain $L = n * n_r$ number of measurements.

In the next section we describe a technique to model the temporal correlation of the measurement noise from (1.5) and after that we link this model with the sequential Monte Carlo techniques for localisation.

1.2.3 Correlated in Time Measurement Noise

In urban and suburban environment the autocorrelation function of the measurement noise (shadowing component) $v_{\ell j,k}$ from (1.5) can be modeled with the relation [37, 38]

$$c_v(\tau) = \sigma_v^2 \exp\{-\mathrm{v}|\tau|/D_c\}, \tag{1.8}$$

where τ is the time lag, σ_v denotes the standard deviation of the shadowing process, D_c is the effective correlation distance, which is of key importance in a wireless environment and v is the velocity of the mobile node. In [37] is shown that

$$D_c = -\frac{d_{\ell j,k}}{\ln(\varepsilon_D)} \geq 0, \tag{1.9}$$

where ε_D is the correlation coefficient of the shadow process between two mobile nodes separated by the distance $d_{\ell j,k}$. Usually D_c is in the range between 10 meters in urban environment and 500 meters in suburban environment. The value of the standard deviation σ_v varies dependent on the environment and in suburban areas is typically 8 dB [37, 38], whereas in urban environments it is roughly 4 dB.

The shadowing process can be modeled by a first-order autoregressive model (AR) [37, 38]

$$v_{\ell j,k} = a v_{\ell j,k-1} + \phi_k, \tag{1.10}$$

where ϕ_k is a zero mean white Gaussian process with variance $\sigma_\phi^2 = (1 - a^2)\sigma_v^2$. The coefficient a is given by

$$a = \exp(-\mathrm{v}T/D_c), \tag{1.11}$$

where T is the measurement sampling period.

It is assumed that the AR model parameters (correlation coefficient and variance) are known and have typical values for urban and suburban environments. These parameters are experimentally obtained by different authors for urban and suburban environment, e.g. in [37, 38, 52].

1.2.4 Motion and Observation Models for Simultaneous Localisation of Multiple Mobile Nodes

A combined state vector $\boldsymbol{X}_k = \{\boldsymbol{x}'_{1,k}, \ldots, \boldsymbol{x}'_{n,k},\}$ is composed and all states of multiple mobile nodes can be simultaneously estimated. The motion model (1.1)-(1.3) can be generalised to the form

$$\boldsymbol{X}_k = \boldsymbol{f}(\boldsymbol{X}_{k-1}, \mathrm{M_k}, \boldsymbol{U}_\mathrm{k}, \boldsymbol{W}_\mathrm{k}), \tag{1.12}$$

where $\boldsymbol{X}_k \in \mathbb{R}^{n*n_x}$ is the combined system *base* state vector, $\boldsymbol{U}_k \in \mathbb{R}^{n*n_u}$ specifies the command processes for all mobile nodes, and the *modal (discrete) state* $\mathrm{M_k} \in \mathbb{S}$ of the different system modes (regimes). The dimension of the combined system noise vector is $\boldsymbol{W}_k \in \mathbb{R}^{n*n_w}$.

The measurement equation (1.7) can be generalised to

$$\boldsymbol{Z}_k = \boldsymbol{h}(\boldsymbol{X}_k) + \boldsymbol{V}_k, \tag{1.13}$$

$$\boldsymbol{V}_k = a\boldsymbol{V}_{k-1} + \boldsymbol{\Phi}_k, \tag{1.14}$$

where $\boldsymbol{Z}_k \in \mathbb{R}^{n*n_z}$ is a generalised measurement vector, and the generalised noise vector $\boldsymbol{V}_k \in \mathbb{R}^{n*n_z}$ characterises the correlated in time shadowing components; $\boldsymbol{\Phi}_k$ is a $(n*n_z)$-dimensional white noise with covariance matrix $E[\boldsymbol{\Phi}_k \boldsymbol{\Phi}_k^{'}] = \sigma_\phi^2 \boldsymbol{I}$ and $\boldsymbol{I}$ denotes the identity matrix.

Equations (1.12)-(1.14) constitute the whole model for the motion of the mobile nodes and observations with a correlated in time noise.

1.3 Sequential Bayesian Framework

1.3.1 General Filtering Framework

Within the sequential Bayesian framework the localisation of mobile nodes reduces to approximation of the state probability density function (PDF) given a sequence of measurements. According to the Bayes' rule the filtering PDF $p(\boldsymbol{X}_k|\boldsymbol{Z}_{1:k})$ of the state vector $\boldsymbol{X}_k \in \mathbb{R}^{n*n_x}$ given a sequence of sensor measurements $\boldsymbol{Z}_{1:k}$ up to time k can be written as

$$p(\boldsymbol{X}_k|\boldsymbol{Z}_{1:k}) = \frac{p(\boldsymbol{Z}_k|\boldsymbol{X}_k)p(\boldsymbol{X}_k|\boldsymbol{Z}_{1:k-1})}{p(\boldsymbol{Z}_k|\boldsymbol{Z}_{1:k-1},)}, \tag{1.15}$$

where $(\boldsymbol{Z}_k|\boldsymbol{Z}_{1:k-1})$ is the normalising constant. The state *predictive* distribution is given by the Chapman-Kolmogorov equation

$$p(\boldsymbol{X}_k|\boldsymbol{Z}_{1:k-1}) = \int_{\mathbb{R}^{n*n_x}} p(\boldsymbol{X}_k|\boldsymbol{X}_{k-1}) p(\boldsymbol{X}_{k-1}|\boldsymbol{Z}_{1:k-1}) d\boldsymbol{X}_{k-1}. \tag{1.16}$$

The evaluation of the right hand side of (1.15) involves integration which can be avoided in the particle filtering approach [53] by approximating the posterior PDF $p(\boldsymbol{X}_k|\boldsymbol{Z}_{1:k})$ with a set of particles $\boldsymbol{X}_{0:k}^{(i)}$, $i = 1,\ldots,N$ and their corresponding weights $w_k^{(i)}$. Then the posterior density can be written as follows

$$p(\boldsymbol{X}_{0:k}|\boldsymbol{Z}_{1:k}) = \sum_{i=1}^{N} w_k^{(i)} \delta(\boldsymbol{X}_{0:k} - \boldsymbol{X}_{0:k}^{(i)}), \tag{1.17}$$

where $\delta(.)$ is the Dirac delta function, and the weights are normalised such that $\sum_i w_k^{(i)} = 1$.

Each pair $\{\boldsymbol{X}_{0:k}^{(i)}, w_k^{(i)}\}$ characterises the belief that the object is in state $\boldsymbol{X}_{0:k}^{(i)}$. An estimate of the variable of interest is obtained by the weighted sum of particles. Two major stages can be distinguished: *prediction* and *update*. During prediction, each particle is modified according to the state model, including the addition of random noise in order to simulate the effect of the noise on the state. In the update stage, each particle's weight is re-evaluated based on the new data. A *resampling* procedure introduces variety in the particles by eliminating those with small weights and replicating the particles with larger weights such that the approximation in (1.17) still holds. The residual resampling algorithm [54, 55] is applied here. This is a two step process making use of sampling-importance-resampling scheme.

Since the command process of the mobile nodes is unknown, a multiple model auxiliary particle filter (MM AUX-PF) for localisation of the mobile nodes is designed and presented in the next section. Given the set M covering well the possible acceleration values, the unknown accelerations are supposed to evolve as a first-order Markov chain with transition probability matrix $\boldsymbol{\Pi}$. The particles for the base state are generated from the transition prior, according to (1.12)-(1.13) (where the motion model for each mobile is given by (1.1)-(1.3).

1.3.2 Auxiliary Multiple Model Particle Filtering for Localisation

The auxiliary Sampling Importance Resampling (SIR) PF was introduced by Pitt and Shephard [56]. The auxiliary PF draws particles from an importance function which is close as possible to the optimal one. The auxiliary PF introduces an importance function $q(\boldsymbol{X}_k, i^{(j)})_{i=1}^N$ where $i^{(j)}$ refers to the index of the particle at $k-1$. The filter obtains samples from the joint density $p(\boldsymbol{X}_k, i|\boldsymbol{Z}_{1:k})$ and then omits the index i in the pair $(\boldsymbol{X}_k, i)$ to produce a sample $\{\boldsymbol{X}_k^{(i)}\}_{i=1}^N$ from the marginalised density

$p(\boldsymbol{X}_k|\boldsymbol{Z}_{1:k})$. The importance density that generates the sample $\{\boldsymbol{X}_k^{(i)}\}_{i=1}^N$ is defined to satisfy the relation [53]

$$q(\boldsymbol{X}_k, i|\boldsymbol{Z}_{1:k}) \propto p(\boldsymbol{Z}_k|\boldsymbol{\mu}_k^{(i)})p(\boldsymbol{X}_k|\boldsymbol{X}_{k-1}^{(i)})w_{k-1}^{(i)}, \tag{1.18}$$

where $\boldsymbol{\mu}_k^{(i)}$ is some characteristic of $\boldsymbol{X}_k$ given $\boldsymbol{X}_{k-1}^{(i)}$ (e.g., the mean or median).

The selection of the most promising particles is carried out by sampling from a multinomial distribution where the number of possible outcomes is N^{out}. The auxiliary PF [56] resamples the predicted particles to select which particles to use in the prediction and measurement update.

For the purposes of mobile node localisation we propose an auxiliary MM PF. The MM AUX-PF represents the PDF $p(\boldsymbol{X}_k, i, \mathrm{M}_k|\boldsymbol{Z}_{1:k})$ where i refers to the i-th particle at $k-1$ and $\mathrm{M_k}$ is the set of acceleration levels, defined as in (1.4). After marginalisation, the representation of $p(\boldsymbol{X}_k|\boldsymbol{Z}_{1:k})$ can be obtained.

Similarly to [34], the joint probability density function $p(\boldsymbol{X}_k, i, \mathrm{M}_k|\boldsymbol{Z}_{1:k})$ can be written using the Bayesian rule as:

$$\begin{aligned} &p(\boldsymbol{X}_k, i, \mathrm{M_k}|\boldsymbol{Z}_{1:k}) \propto p(\boldsymbol{Z}_k|\boldsymbol{X}_k)p(\boldsymbol{X}_k, i, \mathrm{M}_k|\boldsymbol{Z}_{1:k-1}) \\ =&p(\boldsymbol{Z}_k|\boldsymbol{X}_k)p(\boldsymbol{X}_k|\boldsymbol{X}_{k-1}^{(i)}, \mathrm{M}_k)p(\mathrm{M}_k|\mathrm{M}_{k-1}^{(i)})w_{k-1}^{(i)}, \end{aligned} \tag{1.19}$$

where $p(\mathrm{M}_k|\mathrm{M}_{k-1})$ is an element of the transition probability matrix $\boldsymbol{\Pi}$. Since sampling directly from $p(\boldsymbol{X}_k, i, \mathrm{M}_k|\boldsymbol{Z}_{1:k})$ is difficult, the following importance function $q(\boldsymbol{X}_k, i, \mathrm{M}_k|\boldsymbol{Z}_{1:k})$ is introduced

$$q(\boldsymbol{X}_k, i, \mathrm{M}_k|\boldsymbol{Z}_{1:k}) \propto p(\boldsymbol{Z}_k|\boldsymbol{\mu}_k^{(i)}(\mathrm{M}_k))p(\boldsymbol{X}_k|\boldsymbol{X}_{k-1}^{(i)}, \mathrm{M}_k)p(\mathrm{M}_k|\mathrm{M}_{k-1}^{(i)})w_{k-1}^{(i)}, \tag{1.20}$$

where

$$\boldsymbol{\mu}_k^{(i)}(\mathrm{M}_k) = E\left(\boldsymbol{X}_k|\boldsymbol{X}_{k-1}^{(i)}, \mathrm{M}_k\right). \tag{1.21}$$

The importance density $q(\boldsymbol{X}_k, i, \mathrm{M}_k|\boldsymbol{Z}_{1:k})$ differs from (1.19) only in the first factor. Marginalisation over $\boldsymbol{X}_k$ yields

$$q(i, \mathrm{M}_k|\boldsymbol{Z}_k) \propto p(\boldsymbol{Z}_k|\boldsymbol{\mu}_k^{(i)}(\mathrm{M}_k))p(\mathrm{M}_k|\mathrm{M}_{k-1}^{(i)}).w_{k-1}^{(i)}. \tag{1.22}$$

By using (1.22) a random sample from the density $q(\boldsymbol{X}_k, i, \mathrm{M}_k|\boldsymbol{Z}_{1:k})$ can be obtained as follows. First, a sample $\left\{i^{(j)}, \mathrm{M}_k^{(j)}\right\}_{j=1}^N$ is drawn from the multinomial distribution $q(i, \mathrm{M}_k|\boldsymbol{Z}_{1:k})$, (1.22), by splitting each of the N particles at $k-1$ into r groups. Each of the $N*r$ particles is assigned a weight proportional to the right hand site of (1.22). Next, a sample $\left\{\boldsymbol{X}_k^{(j)}\right\}_{j=1}^N$ from the joint density $q(\boldsymbol{X}_k, i, \mathrm{M}_k|\boldsymbol{Z}_{1:k})$ is

generated from $p(\boldsymbol{X}_k|\boldsymbol{X}_{k-1}^{(ij)}, \mathrm{M}_k^{(j)})$. To use the samples $\left\{\boldsymbol{X}_k^{(j)}, i^j, \mathrm{M}_k^{(j)}\right\}_{j=1}^{N}$ to characterise the density $p(\boldsymbol{X}_k, i, \mathrm{M}_k|\boldsymbol{Z}_{1:k})$, we attach to each particle the weight

$$w_k^{(j)} = \frac{p(\boldsymbol{Z}_k|\boldsymbol{X}_k^{(j)})}{p(\boldsymbol{Z}_k|\mu_k^{(ij)}(\mathrm{M}_k))}, \tag{1.23}$$

which represents the ratio of (1.20) and (1.19). By omitting the $\left\{i^{(j)}, \mathrm{M}_k^{(j)}\right\}$ components from the triplet sample $\left\{\boldsymbol{X}_k^{(j)}, i^{(j)}, \mathrm{M}_k^{(j)}\right\}_{j=1}^{N}$, we have representation of the marginalised density $p(\boldsymbol{X}_k|\boldsymbol{Z}_{1:k})$, i.e.

$$p(\boldsymbol{X}_k|\boldsymbol{Z}_{1:k}) \approx \sum_{j=1}^{N} w_k^{(j)} \delta(\boldsymbol{X}_k - \boldsymbol{X}_k^{(j)}). \tag{1.24}$$

The conditional mean $\boldsymbol{\mu}_k^{(i)}(\mathrm{M}_k^{(i)})$ for each particle in the MM AUX-PF comprises the mean vectors of all mobile nodes. The following deterministic mobility equation is used to calculate the mean for each mobile node:

$$\boldsymbol{x}_k = \boldsymbol{A}(T, \alpha)\boldsymbol{x}_{k-1} + \boldsymbol{B}_u(T)\boldsymbol{u}_k. \tag{1.25}$$

The whole MM AUX-PF for mobile nodes localisation is presented as Algorithm 2. The MM AUX-PF takes into account speed constraints, i.e., the speed of each mobile node cannot exceed the maximum value $V_{\max}$. Finally, resampling is performed only when the efficient number of particles, N_{eff} is smaller than a given threshold N_{thresh}.

1.3.3 Approaches to Deal with the Time Correlated Measurement Noise

The time correlation in the measurements can be taken with the account with the following two approaches described below [40].

Approach 1. One approach to overcome the problem with correlated measurement noise is to augment the mobile state $\boldsymbol{x}_k$ with the noise $\boldsymbol{v}_k$. Then the localisation algorithm (MM AUX-PF) described in Subsection 1.3.2 can be applied to the whole augmented state vector of size $n*(n_x+n_z)$ (comprising the state vectors of the mobile nodes and measurement noise). This algorithm with the state vector augmented with the correlated noise is referred to as a MM-AUX PF with augmented state (AS).

Approach 2. Another decorrelation technique introduces the following "artificial measurement": $\bar{\boldsymbol{z}}_k = \boldsymbol{z}_k - a\boldsymbol{z}_{k-1}$. The measurement equation can then be written in the form

Algorithm 2. A Multiple Model Auxiliary PF for Mobile Nodes Localisation

Initialisation

I. $k = 0$, for $i = 1, \ldots, N$,
Generate samples $\{\boldsymbol{X}_0^{(i)} \sim p(\boldsymbol{X}_0), \mathrm{M}_0^{(i)} \sim P_0(\mathrm{M})\ \}$,
and set initial weights $w_0^{(i)} = 1/N$.

II. For $k = 1, 2, \ldots,$
(1) For $i = 1, \ldots, N * r$,
- Calculate the conditional mean:

$$\boldsymbol{\mu}_k^{(i)}(\mathrm{M}_k) = E\left(\boldsymbol{X}_k | \boldsymbol{X}_{k-1}^{(i)}, \mathrm{M}_k\right) \text{ for every } \mathrm{M}_k \in \mathbb{S}$$

(2) Generate $\left\{i^j, \mathrm{M}_k^{(j)}\right\}, j = 1, \ldots, N$ by sampling from $q(i, \mathrm{M}_k | \boldsymbol{Z}_{1:k})$,
where $q(i, \mathrm{M}_k | \boldsymbol{Z}_{1:k}) \propto p(\boldsymbol{Z}_k | \boldsymbol{\mu}_k^{(i)}(\mathrm{M}_k)) p(\mathrm{M}_k | \mathrm{M}_{k-1}^{(i)}) w_{k-1}^{(i)}$.
(3) ***Prediction Step***
For $j = 1, \ldots, N$, predict the particles according to
$\boldsymbol{X}_k^{(j)} = f(\boldsymbol{X}_{k-1}^{(i^j)}, \mathrm{M}_k^{(j)}, \boldsymbol{w}_k^{(j)})$
with noise realisations $\boldsymbol{w}_k^{(j)} \sim \mathcal{N}(0, \boldsymbol{Q})$. Impose the speed constraints.

(4) ***Measurement update***
For $j = 1, \ldots, N$ compute the weights
$w_k^{(j)} = p(\boldsymbol{Z}_k | \boldsymbol{X}_k^{(j)}) / p(\boldsymbol{Z}_k | \boldsymbol{\mu}_k^{(i^j)}(\mathrm{M}_k))$.
Normalise the weights: $\widetilde{w}_k^{(j)} = w_k^{(j)} / \sum_{j=1}^N w_k^{(j)}$

(5) ***Output estimate***
The posterior mean $E[\boldsymbol{X}_k | \boldsymbol{z}_k]$

$$\hat{\boldsymbol{X}}_k = \sum_{j=1}^N \widetilde{w}_k^{(j)} \boldsymbol{X}_k^{(j)}.$$

(6) ***Resampling step***:
Compute the effective sample size
$N_{eff} = 1 / \sum_{j=1}^N (\widetilde{w}_k^{(j)})^2$,

Resample if $N_{eff} < N_{thresh}$
* For $i = 1, \ldots, N$, set $w_k^{(i)} = 1/N$.

$$\bar{\boldsymbol{z}}_k = \boldsymbol{z}_k - a\boldsymbol{z}_{k-1} \tag{1.26}$$

$$= \boldsymbol{h}(\boldsymbol{x}_k) + \boldsymbol{v}_k - a\left[\boldsymbol{h}(\boldsymbol{x}_{k-1}) + \boldsymbol{v}_{k-1}\right] \tag{1.27}$$

$$= \boldsymbol{h}(\boldsymbol{x}_k) - a\boldsymbol{h}(\boldsymbol{x}_{k-1}) + \bar{\boldsymbol{v}}_k. \tag{1.28}$$

The noise $\bar{\boldsymbol{v}}_k = \boldsymbol{v}_k - a\boldsymbol{v}_{k-1}$ in the new measurement equation is white but correlated with the process noise. The cross-correlation between two noise sequences can be eliminated by a procedure, given in [47]. In most practical algorithms this cross-correlation is omitted due to the little performance degradation. Thus the measurement equation in the case of one mobile node can be modified to

$$\bar{\boldsymbol{z}}_k = \bar{\boldsymbol{h}}(\boldsymbol{x}_k) + \bar{\boldsymbol{v}}_k, \tag{1.29}$$

where $\bar{\boldsymbol{h}}(\boldsymbol{x}_k) = \boldsymbol{h}(\boldsymbol{x}_k) - a\boldsymbol{h}(\boldsymbol{x}_{k-1})$.

The MM-AUX PF algorithm with decorrelation is referred to as with an artificial measurement (AM).

1.4 Estimation of the Measurement Noise Parameters

The parameters of the RSSI measurement noise vary significantly depending on the environment: urban, suburban or rural. This causes difficulties to most of localisation techniques since their accuracy depends to a high extent on the noise parameters. In practice, the noise characteristics of the received signal strengths can vary in a large range, e.g., between 3dB and 24dB depending on the environment: urban or semi-urban, different meteorological conditions (snow, rain), presence of obscuration or attenuation of the signals and are typically correlated [37]. A relatively small number of works consider the noise parameter estimation. Between the related works we have to mention [41] and [57]. In [57] the noise parameter estimation is performed with a single Dirichlet process and in [58] based on a mixture of Dirichlet processes. In [41] a Gibbs sampling approach is proposed for estimating the unknown noise parameters of the measurement noise based on batch measurements and next the estimated parameters are fed to the localisation techniques.

The next section presents a Gibbs sampling algorithm for estimating the unknown measurement noise parameters. The localisation of mobile nodes is performed after that with these noise parameter estimates embedded in the MM AUX-PF. The proposed approach deals successfully with the highly nonlinear measurement models with non-Gaussian measurement errors, can incorporate physical constraints and possibly communications among frequently manoeuvring mobile nodes in the form of additional measurements.

The noise $\boldsymbol{v}_k$ characterises the shadowing components, assumed to be uncorrelated in time and with unknown parameters. One simple, but effective solution to the localisation problem with unknown noise parameters is to model the measurement noise as a n_{mix}-component Gaussian mixture

$$\boldsymbol{v}_k \sim \sum_{i=1}^{n_{mix}} \pi_i \mathcal{N}(\mu_i, \sigma_i^2), \tag{1.30}$$

where μ_i and σ_i^2 are the mean and variance of the mixture component i and $\boldsymbol{\pi} = (\pi_1, \ldots, \pi_{n_{mix}})$ is a vector of mixture weights π_i (constrained to be non-negative and with unit sum). The features of the measurement process and environment, the availability of missed or false observations can be captured well by the mixture.

The mixture parameters are estimated by introducing a hierarchical data structure of the mixture model and accounting for the missing data. In particular, Markov chain Monte Carlo (MCMC) techniques are very efficient inference methods. For hierarchical models, Gibbs sampling has proved to be the most effective among various MCMC methods. Gibbs sampling is especially appropriate for the localisation

problem under unknown measurement parameters. The mixture can be composed of different distributions such as t, Student or Gaussian. We choose Gaussian components since they lead easily to tractable solutions and can model well complex probability density functions even with a small number of components [59].

We estimate the measurement noise parameters with the Gibbs sampler presented in Section 1.5 and next the mobile nodes self-localisation is performed by the Multiple Model Auxiliary Particle Filter given in Section 1.3.

1.5 Gibbs Sampling for Noise Parameter Estimation

We suggest to estimate the unknown noise parameters of the measurement model (1.5)-(1.29) with Gibbs sampling (GS), a special form of Bayesian sampling benefitting from the hierarchical structure of the model [60]. Given the observation of a T_m-dimensional vector $\boldsymbol{\eta} = (\eta_1, \ldots, \eta_{T_m})' \in \mathbb{R}^{T_m}$ of independent random variables (corresponding to the RSSI measurement error $\boldsymbol{v} = (v_{\ell j,1}, v_{\ell j,2}, \ldots, v_{\ell j,T_m})$[1]), the mixture [61] is formed

$$F(\eta_t) = \sum_{i=1}^{n_{mix}} \pi_i F_i(\eta_t),\ t = 1, \ldots, T_m, \tag{1.31}$$

where the densities $F_i,\ i = 1, \ldots, n_{mix}$ are known or are known up to a parameter. The weight vector $\boldsymbol{\pi} = (\pi_1, \ldots, \pi_{n_{mix}})$ has non-negative components π_i which sum is equal to 1. We are representing the measurement noise by a Gaussian mixture model (GMM): the density $F_i(\eta_t)$ is then Gaussian, $\mathcal{N}(\mu_i, \sigma_i^2)$, where μ_i and σ_i^2 are the mean and variance of the i-th mixture component. The unknown parameters and weights of the GMM, denoted by $\boldsymbol{\theta} = (\theta_1, \ldots, \theta_{r_m}) = \left(\mu_1, \sigma_1^2, \ldots, \mu_{n_{mix}}, \sigma_{n_{mix}}^2, \pi_1, \ldots \pi_{n_{mix}}\right)$ are iteratively estimated.

According to [61], the mixture model can be represented in terms of missing (or incomplete) data. The model is *hierarchical* with the true parameter vector $\boldsymbol{\theta}$ of the mixture, on the top level and on the bottom are the observed data. The GS relies additionally on the availability of all complete conditional distributions of the elements of $\boldsymbol{\theta}$, breaking down $\boldsymbol{\theta}$ into r_m subsets. It generates $\theta_j, j = 1, \ldots, r_m$ conditional on all the other parameters, increasing in this way the number of conditional simulations. The details of the GS algorithm can be found in a number of publications [61, 62]. The n_{mix}-dimensional vectors $\boldsymbol{\delta}_t$, $t = 1,\ 2,\ \ldots, T_m$ with components $\delta_{t,i} \in \{0, 1\},\ i = 1, 2,\ \ldots, n_{mix}$ and $\sum_{i=1}^{n_{mix}} \delta_{t,i} = 1$ are defined to indicate that the measurement η_t has density $F_i(\eta_t)$. Next, the missing data distribution depends on $\boldsymbol{\theta}$, $\boldsymbol{\delta} \sim p(\boldsymbol{\delta}|\boldsymbol{\theta})$. The observed data, $\boldsymbol{\eta} \sim p(\boldsymbol{\eta}|\boldsymbol{\theta}, \boldsymbol{\delta})$, are at the bottom level. Bayesian sampling iteratively generates parameter vectors $\boldsymbol{\theta}^{(u)}$ and missing data $\boldsymbol{\delta}^{(u)}$ according to $p(\boldsymbol{\theta}|\boldsymbol{\eta}, \boldsymbol{\delta}^{(u)})$ and $p(\boldsymbol{\delta}|\boldsymbol{\eta}, \boldsymbol{\theta}^{(u+1)})$. Here, u indexes the current iteration.

[1] From the measurement model (1.5), estimated positions (x_ℓ, y_ℓ), the estimated distance $d_{\ell,j}$ and with known transmission constant $\kappa_{\ell,j}$, noise realisations $v_{\ell j,1:T_m}$ are found which serve as measurements to GS.

It is proven in [61], that Bayesian sampling produces an ergodic Markov chain $(\boldsymbol{\theta}^{(u)})$ with stationary distribution $p(\boldsymbol{\theta}|\boldsymbol{\eta})$. After u_0 initial (warming up) steps, a set of U samples $\boldsymbol{\theta}^{(u_0+1)}, \ldots, \boldsymbol{\theta}^{(u_0+U)}$ are approximately distributed as $p(\boldsymbol{\theta}|\boldsymbol{\eta})$. Due to ergodicity, averaging can be made with respect to time and the empirical mean of the last U values can be used as an estimate of $\boldsymbol{\theta}$.

The choice of prior distributions and their hyperparameters is a first, important step of the design of a Gibbs sampler. Conjugate prior distributions [2] are chosen (as in most cases in the literature) since this simplifies the implementation. Since the conjugate prior of $\boldsymbol{\pi}$ is a *Dirichlet* distribution (DD), $\mathscr{D}(\alpha_1,\ldots,\alpha_{n_{mix}})$ [61], $\boldsymbol{\pi}$ is generated according to the DDs with parameters, depending on the missing data. The conjugate priors for σ_i^2 and $\mu_i|\sigma_i^2, i=1,\ldots,n_{mix}$ are the *Inverse Gamma*($\mathscr{IG}$) and *Gaussian* distribution respectively, as recommended in [61]:

$$\boldsymbol{\pi} \sim \mathscr{D}(\alpha_1,\ldots,\alpha_{n_{mix}}), \tag{1.32}$$

$$\sigma_i^2 \sim \mathscr{IG}(\nu_i, s_i^2), \tag{1.33}$$

$$\mu_i|\sigma_i^2 \sim \mathscr{N}(\xi_i, \sigma_i^2/n_i). \tag{1.34}$$

Here, $\alpha_i, \nu_i, s_i^2, \xi_i$, and $n_i, i \in 1,\ldots,n_{mix}$ are the corresponding hyperparameters.

Starting with an initial parameter vector $\boldsymbol{\theta}^{(0)}$, the following *iterative algorithm* is implemented: at the iteration $u, u = 0,1,2,\ldots$

a) *generate* $\boldsymbol{\delta}^{(u)} \sim p(\boldsymbol{\delta}|\boldsymbol{\eta},\boldsymbol{\theta}^{(u)})$ from a multinomial distribution with weights proportional to the observation likelihoods, i.e. $p(\delta_{ti}^{(u)}) \propto \pi_i^{(u)} \mathscr{N}\left(\eta_t; \mu_i^{(u)}, \sigma_i^{(u)^2}\right)$;

b) *generate* $\boldsymbol{\pi}^{(u+1)} \sim p(\boldsymbol{\pi}|\boldsymbol{\eta},\boldsymbol{\delta}^{(u)})$:

$$\boldsymbol{\pi}^{(u+1)} \sim \mathscr{D}\left(\alpha_1 + \Delta_1^{(u)}, \ \ldots, \ \alpha_{n_{mix}} + \Delta_{n_{mix}}^{(u)}\right)$$

where $\Delta_i^{(u)} = \sum_{t=1}^{T_m} \delta_{t,i}^{(u)}$ is the number of observations allocated to the mixture component i;

c) *generate* $\mu_i^{(u+1)}|\sigma_i^{(u)^2} \sim \mathscr{N}\left(\xi_i, \sigma_i^{(u)^2}/n_i\right)$:

$$\mu_i^{(u+1)} \sim \mathscr{N}\left(\frac{n_i\xi_i + \sum_{t=1}^{T_m} \delta_{t,i}^{(u)} \eta_t}{n_i + \Delta_i^{(u)}}, \frac{\sigma_i^{(u)^2}}{n_i + \Delta_i^{(u)}}\right)$$

where ξ_i is the average of the observations attributed to the mixture component i;

d) *generate*

[2] *Conjugate distributions* are distributions that have the same functional form, e.g., the posterior is the same as the prior distribution and the prior is called a conjugate prior for the likelihood. Conjugate priors play an important role since they lead to elegant Bayesian solutions.

$$\sigma_i^{(u+1)^2} \sim \mathscr{IG}\left(\nu_i + \upsilon_i, s_i^2 + \widehat{s}_i^2 + n_i(\xi_i - \mu_i^{(u+1)})^2\right),$$

where $\upsilon_i = 0.5(\Delta_i^{(u)} + 1)$, $s_i^2 = (T_m(n_{mix} - 1))^{-1} \sum_{t=1}^{T_m} (\eta_i - \overline{\eta})^2$, ($\overline{\eta}$ is the empirical mean of the measurement data), $\widehat{s}_i^2 = \sum_{t=1}^{T_m} \delta_{t,i}^{(u)} (\eta_t - \mu_i^{(u+1)})^2$; We consider the additional assumption that $\sigma_i^2 \in [\sigma_{min}^2, \sigma_{max}^2]$. Truncated conjugate priors are still conjugate [61]. Sampling is realised by generating $\sigma_i^{(u)^2}$ from the $\mathscr{IG}$ distribution until $\sigma_i^{(u)^2} \in [\sigma_{min}^2, \sigma_{max}^2]$.

e) *calculate* the output estimate $\hat{\boldsymbol{\theta}} = \frac{1}{U} \sum_{l=1}^{U} \boldsymbol{\theta}^{(u_0+l)}$.

The next section presents results with the Gibbs sampling algorithm.

1.6 Performance Evaluation of the Gibbs Sampling Algorithm for Measurement Noise Parameter Estimation

1.6.1 Measurement Noise Parameter Estimation with Simulated Data

First we consider a scenario where the trajectory of the ℓ-th mobile node is provided by a GPS system, which collects its actual positions during a time interval $t = 1, \ldots, T_m$ with sampling period T. Knowing the distance to the j-th reference node and using the RSSI measurements $z_{\ell j,t}$, the measurement error parameters can be estimated. A sample of measurement errors $v_{\ell j,t}, t = 1, \ldots, T_m$ can be obtained also, if the mobile mode is static for some time interval or if it is moving along a road with known parameters (the route map is available). In the univariate case, where all mobile nodes have the same noise statistics $v_{\ell j,t} = v_t, t = 1, \ldots, T_m$, the noise characteristics can be assessed preliminary, improving in this way the filter performance. GS for estimating mixture parameters is investigated over simulated and real data.

We have selected the following hyperparameters for every $i = 1, \ldots, n_{mix}$: $n_i = 1$, $\nu_i = n_{mix}$, if $\alpha_i = 1$, the Dirichlet distribution reduces to a uniform distribution and the algorithm is initialised with noninformative prior about mixture proportions. The initial values of $\boldsymbol{\theta}^{(0)}$ are chosen based on the prior information about physical restrictions on the parameters: $\sigma_i^{(0)} = 6$ $[dB]$, the bounds of the supplementary assumption $\sigma_i^2 \in [\sigma_{min}^2, \sigma_{max}^2]$ are respectively $[1^2, 20^2]$. Initial mean values $\mu_i^{(0)}$ are calculated based on the observed interval of variation of the data. The initial weights are selected $\pi_i^{(0)} = 1/n_{mix}$. The number of iterations is 250 and the initial "warming up" interval is $u_0 = 100$.

We performed experiments over the scenario shown in Figure 1.1 after evaluating the noise parameters first. A sample of $T_m = 2000$ measurement errors is generated according to the following mixture model with $n_{mix} = 2$ elements:

$v_t \sim 0.2\mathcal{N}(-6.5, 2^2) + 0.8\mathcal{N}(8.0, 4^2)$. The histogram of the modeled measurement errors is presented in Figure 1.2 (a). The two modes are well pronounced on this Figure. The estimated mixture parameters are $\widehat{\boldsymbol{\pi}} = (0.19, 0.81)$, $\widehat{\mu}_1 = -6.9$, $\widehat{\sigma}_1^2 = 4$, $\widehat{\mu}_2 = 8.04$, $\widehat{\sigma}_2^2 = 17$. The mixture PDF approximation of the noise is given in Figure 1.2 (b).

It is assumed that the accelerations of the mobile nodes u_x and u_y can change within the range $[-5,5]$ $[m/s^2]$ and that the command process $\boldsymbol{u}$ takes values among the following acceleration levels $\mathrm{M} = \{(0,0)', (3.5,0)', (0,3.5)', (0,-3.5)', (-3.5,0)'\}$. Thus the number of motion modes is 5. Non-random mobile node trajectories were generated with the dynamic state equation (1.1)-(1.3) without a process noise.

The reference nodes in the scenario from Figure 1.1 are randomly deployed on the observed area. The MM AUX-PF performance with noise statistics estimated by GS is compared with the filter performance with inaccurate noise distributions: in the first case the measurement noise statistics are assumed Gaussian with parameters: $v_t \sim \mathcal{N}(0, \sigma_{mix}^2)$, where $\sigma_{mix}^2 = 6^2$ is the mixture variance, and in the second case $v_t \sim \mathcal{N}(0, 4^2)$, parameters typical for urban environment. The respective position and speed RMSE are given in Figures 1.3 (a) and (b). The experiments show that accurate noise parameters are improving the localisation accuracy for deterministically deployed sensor networks. However, they are especially useful for randomly deployed networks. It can be seen from Figure 1.3 (a) and (b) that the estimation errors are larger where the manoeuvering phases of mobile nodes coincide with the places of sparsely located reference nodes. The peak dynamic errors increase when the information about noise parameters is insufficient. The position and speed root-mean-square errors (RMSEs) are minimum when the filter operates with estimated noise parameters. If the mean (case 2 in Figure 1.3) or mean and variance (case 3) of the noise are unknown, the errors increase progressively. The parameters of the state vector initial distribution $\boldsymbol{x}_{1,0} \sim \mathcal{N}(\boldsymbol{m}_{1,0}, \boldsymbol{P}_{1,0})$ are selected as follows: $\boldsymbol{P}_{1,0} = \mathrm{diag}\{\boldsymbol{P}_{\mathrm{x},0}, \boldsymbol{P}_{\mathrm{y},0}\}$, $\boldsymbol{P}_{x,0} = \boldsymbol{P}_{y,0} = \mathrm{diag}\{30\,[\mathrm{m}]^2, 1\,[\mathrm{m/s}]^2, 0.5\,[\mathrm{m/s^2}]^2\}$, and $\boldsymbol{m}_{1,0}$ contains the exact initial node states. Initial mode probabilities are $\tilde{\mu}_{1,0} = 0.8$ and $\tilde{\mu}_{1,0} = 0.05$ for $i = 2, \ldots, 5$. The transition probability matrix $\boldsymbol{\Pi}$ has diagonal elements: $\Pi_{11} = 0.9, \Pi_{ii} = 0.7$, $i = 2, \ldots, 5$. The other parameters of the algorithm are given in Table 1.

The RMSE combined on both position coordinates are used to assess the closeness of the estimated state parameters to the actual dynamic parameters of mobile nodes over $N_{mc} = 50$ Monte Carlo runs.

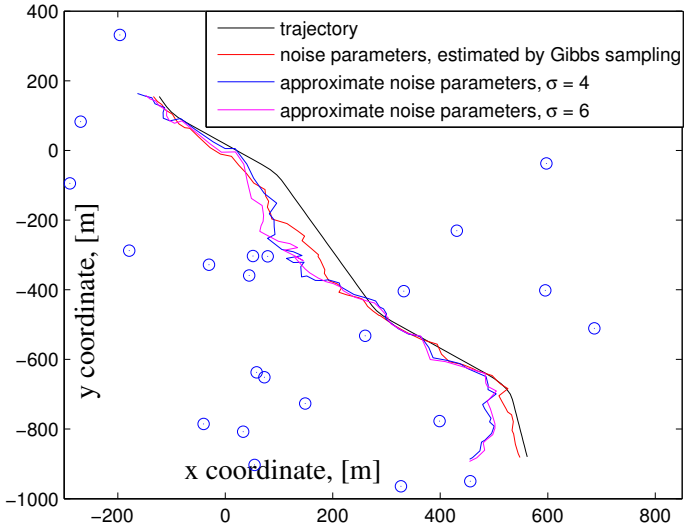

Fig. 1.1. A mobile unit moving in an area covered with randomly deployed wireless sensors with unknown measurement noise characteristics. Estimated trajectories are shown, obtained by the MM AUX-PF: 1. noise parameters estimated with Gibbs Sampling: $v_k \sim \sum_{i=1}^{2} \widehat{\pi}_i \mathcal{N}(\widehat{\mu}_i, \widehat{\sigma}_i^2)$, 2: the measurement noise characteristics are fixed, chosen preliminary as follows: $v_k \sim \mathcal{N}(0, 6^2)$, and respectively, $3: v_k \sim \mathcal{N}(0, 4^2)$

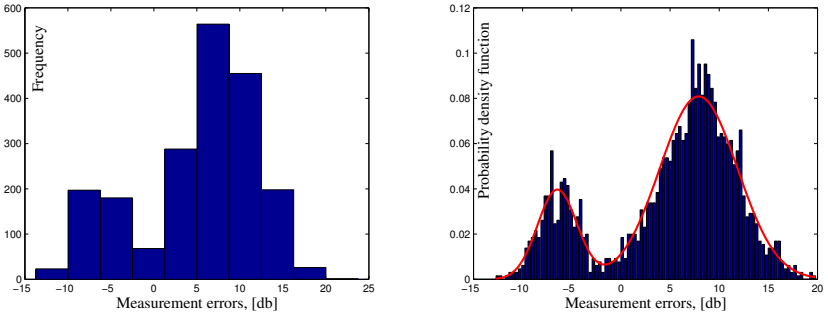

Fig. 1.2. (a) Histogram of the modeled noise, (b) Noise histogram overlayed with mixture density estimate

Table 1. Simulation parameters

Discretisation time step T	1.0 [s]
Correlation coefficient a	0.35
Path loss index γ	4
Transmission power κ	30
Variance σ_w^2 of the noise $\boldsymbol{w}_k$ in (1.1)	0.5^2 $[m/s^2]^2$
Maximum speed $V_{\max}$	45 $[m/s]$
Number of particles	$N = 500$
Threshold for resampling	$N_{thresh} = N/10$
Number of Monte Carlo runs	$N_{mc} = 50$
Variance σ_v^2 of the noise v_k	4^2 [dB]^2

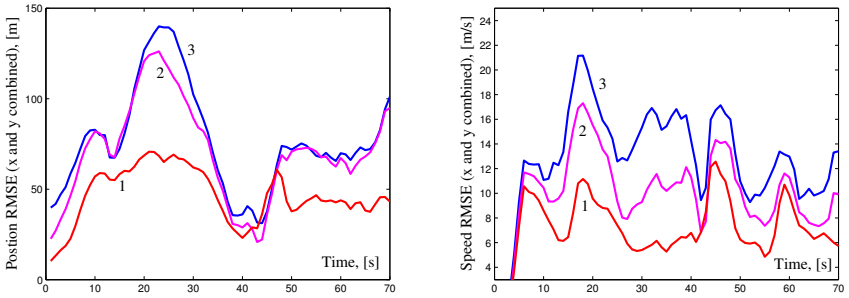

Fig. 1.3. Position RMSE combined (for x and y) and speed RMSEs (for $\dot{x}$ and $\dot{y}$): $1: v_k \sim \sum_{i=1}^{2} \widehat{\pi}_i \mathcal{N}(\widehat{\mu}_i, \widehat{\sigma}_i^2)$, $2: v_k \sim \mathcal{N}(0, 6^2)$, $3: v_k \sim \mathcal{N}(0, 4^2)$

1.6.2 Measurement Noise Parameter Estimation with Real Data

The performance of the GS algorithm has been investigated with real RSSIs, collected from base stations (BSs), by HW Communications Ltd., in Glasgow, United Kingdom. The mobile station was a vehicle driving in the city centre and its trajectory is shown on Figures 1.4 and 1.5. The vehicle movement contains both patterns with sharp manoeuvres and rectilinear motion, including a stretch at the end where the vehicle is parked. Additional information for the road is included as position constraints in the algorithms.

More than 400 BSs are available in the area where the car operated. However, only data from the six with the highest RSSIs were provided to the localisation algorithm. Also a GPS system collected the actual positions of the moving mobile, for the purposes of validating the performance of the developed algorithms. The data from three BSs are used to evaluate the noise characteristics. The sample size is $T_m = 800$. The noise histogram and density estimate, obtained by fitting the mixture parameters to the data are presented in Figure 1.6 (a), (b) and (c). The number of iterations and the "warming up" bound are selected to be 550 and 450 respectively. The initial standard deviation is chosen as $\sigma^{(0)} = 1.5$ $[dB]$, with an additional sampling restriction of $\sigma_{min}^2 = 0.001^2$ and $\sigma_{max}^2 = 10^2$. The actual trajectory of the mobile is shown on Figure 1.5 and the estimated trajectories are given on Figure 1.7 both without and with GS for estimating the noise parameters. The position RMSE is presented on Figure 1.8.

For the GS algorithm when the data histograms have clearly differentiated modes (such as in Figure 1.2), the number of mixture components can be easily determined and this facilitates the mixture parameters evaluation. When the modes are difficult to distinguish (such as in Figure 1.6 (c)), a small number of mixture components can be used. However, this is not an obstacle in the present application. As a result from the GS, the following estimates are obtained for the noise parameters of the RSSI from the three base stations: BS1 ($n_{mix} = 2$) and mixture estimates $\hat{\boldsymbol{\pi}} = (0.2, 0.79)'$,

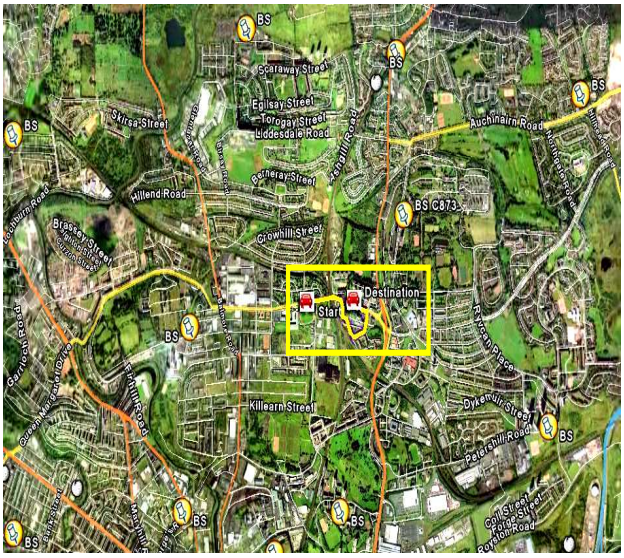

Fig. 1.4. The area in Glasgow, United Kingdom, where the vehicle is moving. The nearest BSs, the start and destination positions are indicated on the map.

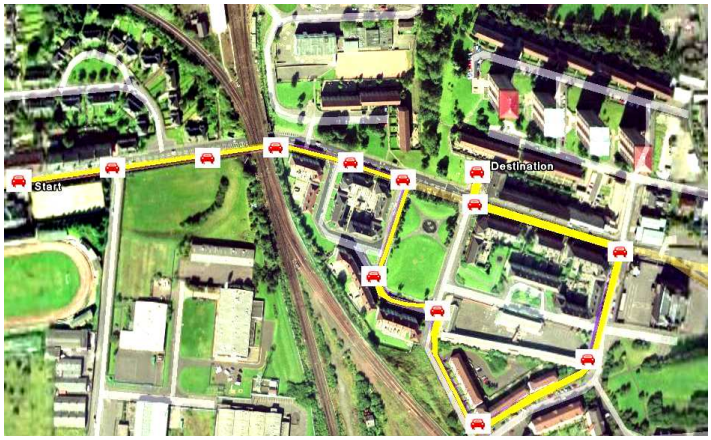

Fig. 1.5. Actual trajectory of the mobile node

$\hat{\boldsymbol{\mu}} = (-5.4, 1.46)'$, $\sigma_{v,1} = 4.15, \sigma_{v,2} = 4.7$; BS2 ($n_{mix} = 3$) with mixture estimates $\hat{\boldsymbol{\pi}} = (0.07, 0.5, 0.4)'$, $\hat{\boldsymbol{\mu}} = (-16.25, -3.26, 5.02)'$, $\sigma_{v,1} = 3.22$, $\sigma_{v,2} = 17.59$, $\sigma_{v,3} = 5.6$; BS3 ($n_{mix} = 2$) with mixture estimates $\hat{\boldsymbol{\pi}} = (0.48, 0.52)'$, $\sigma_{v,1} = 20.27$, $\sigma_{v,1} = 25.6$.

The GS computational time in the case of 550 iterations and sample size $T_m = 800$ is approximately 30 seconds on a conventional PC (AMD Athlon(tm) 64 Processor

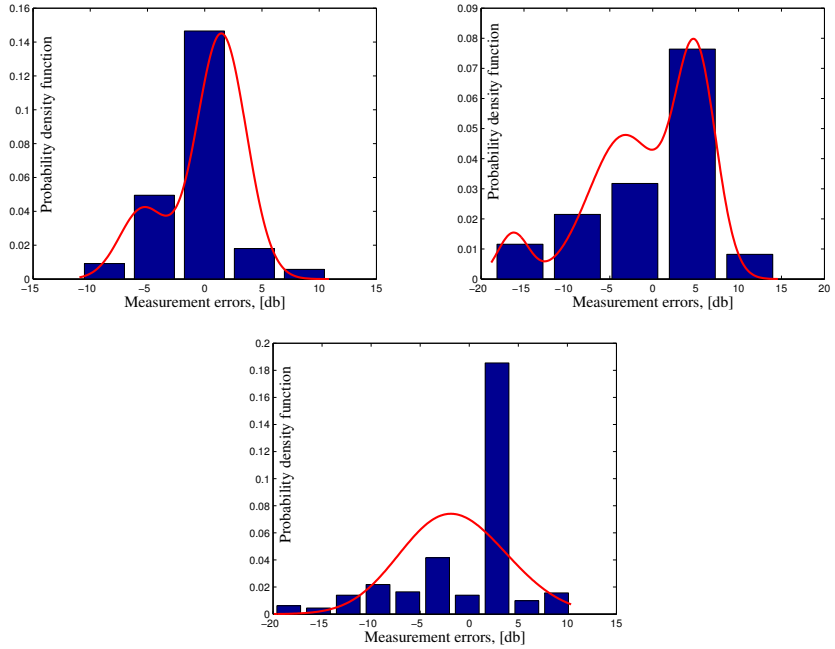

Fig. 1.6. Noise histogram and density estimate with $n_{mix} = 2$ components for: (a) BS1, (b) BS2, (c) BS3

1.81 GHz). With a sample size $T_m = 2000$, the computational time is less than 2 minutes.

1.7 Performance Evaluation of the Multiple Model Auxiliary Particle Filter

Two cases have been investigated: for urban and suburban environment. In suburban environment, the correlation coefficient of the shadow process can be regarded as a constant for a wide range of velocities of the mobile [38]. Typical values of the correlation coefficient and shadow process are assumed, as suggested in the literature [37].

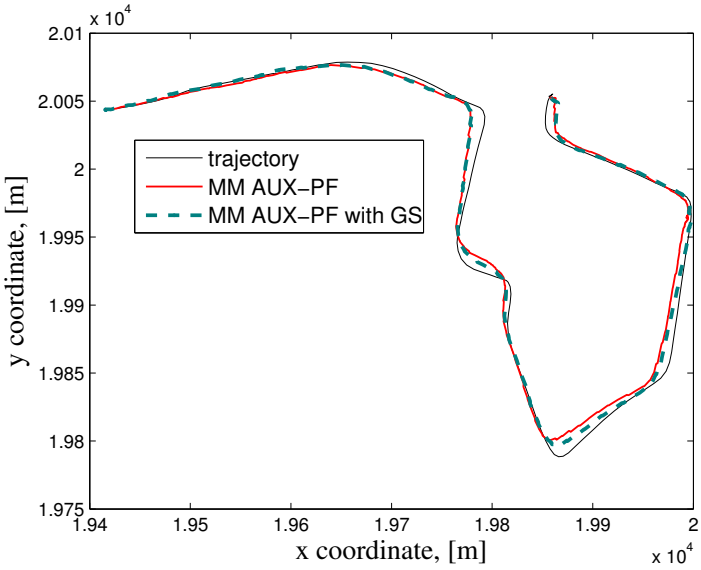

Fig. 1.7. Actual and estimated trajectories obtained by the MM AUX-PF: 1: $v_k \sim \mathcal{N}(0,6^2)$**, 2. noise parameters estimated with the GS, for** BS_1**,** $v_k \sim \sum_{i=1}^{2} \widehat{\pi}_i \mathcal{N}(\widehat{\mu}_i, \widehat{\sigma}_i^2)$**, for** BS_2 $v_k \sim \sum_{i=1}^{3} \widehat{\pi}_i \mathcal{N}(\widehat{\mu}_i, \widehat{\sigma}_i^2)$ **and for** BS_3**,** $v_k \sim \sum_{i=1}^{2} \widehat{\pi}_i \mathcal{N}(\widehat{\mu}_i, \widehat{\sigma}_i^2)$**.**

1.7.1 Results with Simulated Data

Testing scenario. A sensor deployment architecture is considered, similar to the presented in [35]. Three mobile nodes are moving in an urban area well covered with a wireless sensor network (Figure 1.9). Each mobile node can measure the RSSI to each of the reference nodes, but only the three RSSIs with the highest strength are used for localisation.

The MM AUX-PF AS is run for estimating the augmented state vector, consisting of three individual mobile state vectors. Figure 1.9 presents the actual and estimated trajectories of the three mobile nodes. The actual speed of the mobiles is shown in Figure 1.10.

The parameters of the individual state vector initial distribution $\boldsymbol{x}_{i,0} \sim \mathcal{N}(\boldsymbol{m}_{i,0}, \boldsymbol{P}_{i,0})$ are selected as follows: $\boldsymbol{P}_{i,0} = \text{diag}\{\boldsymbol{P}_{\text{x},0}, \boldsymbol{P}_{\text{y},0}\}$, with

$$\boldsymbol{P}_{x,0} = \boldsymbol{P}_{y,0} = \text{diag}\{30\,[\text{m}]^2, 1\,[\text{m/s}]^2, 0.5\,[\text{m/s}^2]^2\},\ i = 1,2,3$$

and $\boldsymbol{m}_{i,0}$ contains the exact initial node states. Initial mode probabilities are $\tilde{\mu}_{1,0} = 0.8$ and $\tilde{\mu}_{i,0} = 0.05$ for $i = 2,\ldots,5$. The transition probability matrix Π has the following diagonal elements: $\Pi_{11} = 0.9, \Pi_{ii} = 0.7,\ i = 2,\ldots,5$ and the off-diagonal

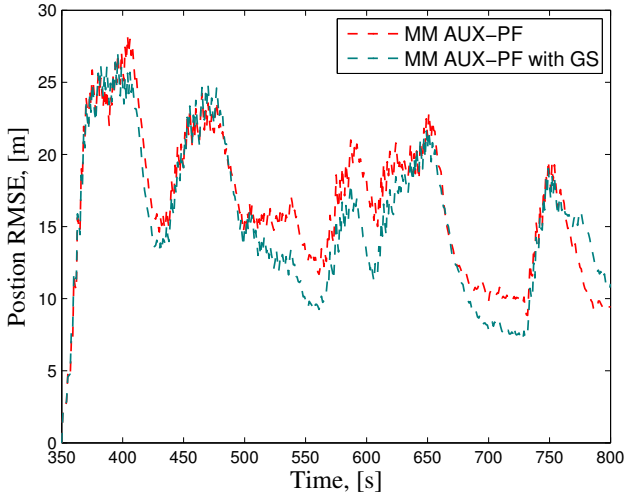

Fig. 1.8. Position RMSE (combined for x and y) of the MM AUX-PF: 1: $v_k \sim \mathcal{N}(0,6^2)$, 2. noise parameters estimated with the GS, for BS_1, $v_k \sim \sum_{i=1}^{2} \widehat{\pi}_i \mathcal{N}(\widehat{\mu}_i, \widehat{\sigma}_i^2)$, for BS_2 $v_k \sim \sum_{i=1}^{3} \widehat{\pi}_i \mathcal{N}(\widehat{\mu}_i, \widehat{\sigma}_i^2)$ and for BS_3, $v_k \sim \sum_{i=1}^{2} \widehat{\pi}_i \mathcal{N}(\widehat{\mu}_i, \widehat{\sigma}_i^2)$.

elements (e.g., $\Pi_{i,1} = 0.025,\ i = 2,\ldots,5,\ \Pi_{i,2} = 0.07,\quad i = 3,\ldots,5$) are chosen equal in each row to guarantee that the some in each row is equal to one. The noise correlation coefficient was assumed to be equal to a typical value for urban environment, 0.25. The correlated measurement noises are generated by means of Cholesky factorisation.

The other parameters of the algorithm are given in Table 2.

Table 2. Simulation parameters for urban environment

Discretisation time step T	1.0 [s]
Correlation coefficient a	0.25
Path loss index γ	5
Transmission power κ	30
Variance σ_w^2 of the noise $\boldsymbol{w}_k$ in (1.1)	$0.5^2\ [m/s^2]^2$
Maximum speed $V_{\max}$	45 $[m/s]$
Number of particles of the MM AUX-PF	$N = 500$
Threshold for resampling	$N_{thresh} = N/10$
Number of Monte Carlo runs	$N_{mc} = 50$
Variance σ_v^2 of the measurement noise v_k	4^2 [dB]^2

It is assumed that the accelerations of the mobile nodes u_x and u_y can change within the range $[-5,5]$ $[m/s^2]$ and that the command process $\boldsymbol{u}$ takes values among the following acceleration levels M$=\{(0,0)', (3.5,0)', (0,3.5)', (0,-3.5)', (-3.5,0)'\}$.

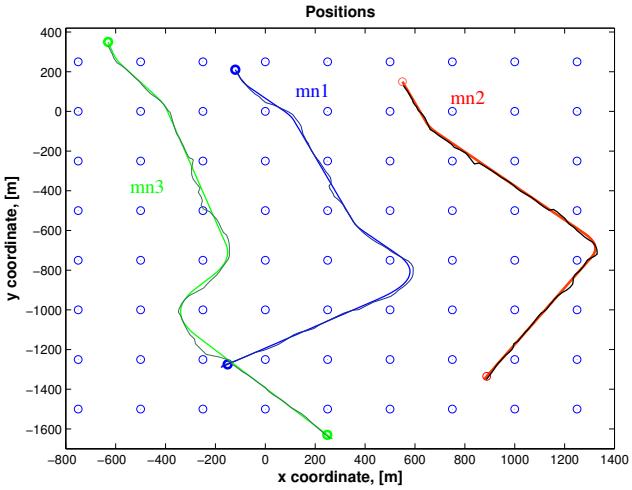

Fig. 1.9. Testing scenario 1: three mobile nodes (mn1, mn2 and mn3) moving in an area covered with a wireless sensor network. The sensors are uniformly deployed and form a rectangular grid.

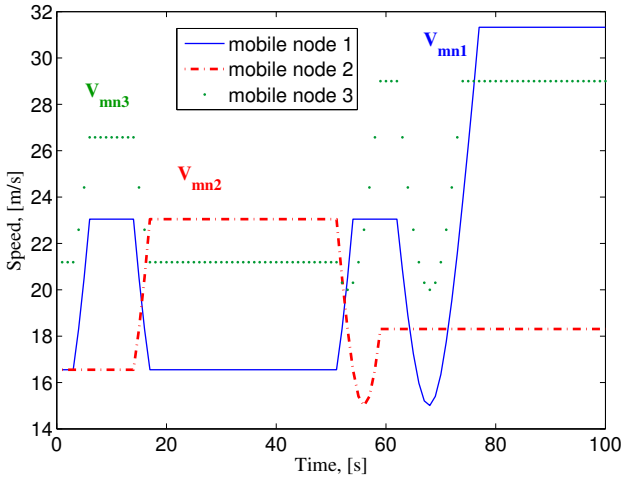

Fig. 1.10. Actual speeds of the three manoevring mobile nodes

Thus the number of motion modes is $r = 5$. Non-random mobile node trajectories were generated with the dynamic state equation (1.1)-(1.3) without process noise. The initial state vectors are as follows: $\hat{\boldsymbol{x}}_{1,0} = (-120, 7, 0, 210, -15, 0)'$,

$\hat{\boldsymbol{x}}_{2,0} = (550, 7, 0, 150, -15, 0)'$ and $\hat{\boldsymbol{x}}_{3,0} = (-630, 7, 0, 350, -20, 0)'$. The first mobile node performs 3 short-term manoeuvres with accelerations from the mode set and a longer manoeuvre with a control input $\boldsymbol{u} = (-3.0, 0.0)$, different from the acceleration set. The second mobile node manoeuvres are described by the set of accelerations. The third mobile node performs two consecutive manoeuvres with opposing accelerations. The root-mean-square errors (RMSE) [42] combined on

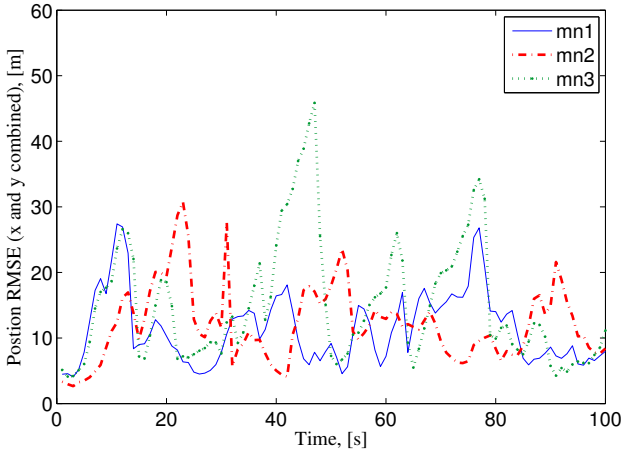

Fig. 1.11. Results for the position RMSE obtained with the MM AUX-PF with an augmented state vector

both position coordinates yield the estimated state parameters to the actual dynamic parameters of each mobile node over $N_{mc} = 50$ Monte Carlo runs. The position and speed RMSEs of the MM AUX-PF with augmented state are shown on Figures 1.11 and 1.12. High position and speed estimates are achieved, with accuracy less than 45m with respect to the mobile nodes position.

1.7.2 Results with Real Data

The performance of the proposed localisation MM-AUX-PF algorithms, with AS and AM, respectively, has been investigated over the same real RSSIs, presented in Section 1.6.2. The mobile station was a vehicle driving in the city centre.

Figure 1.13 shows the actual trajectory of the mobile together with the estimated trajectories and Figure 1.14 gives the respective position RMSEs. With the real RSSIs we compared the performance of: *i*) the MM AUX-PF that does not take

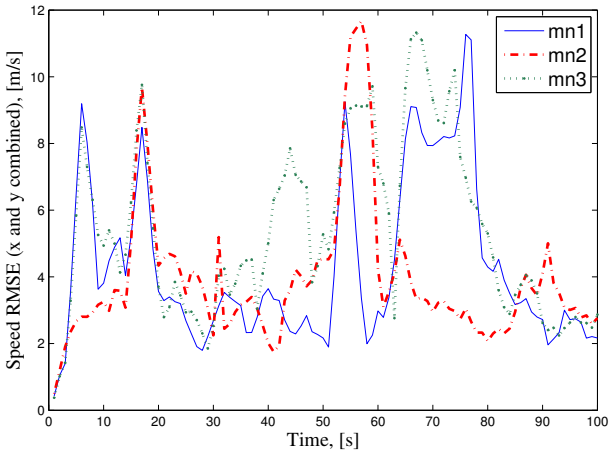

Fig. 1.12. Results for the speed RMSE obtained with the MM AUX-PF with an augmented state

into account the temporal measurement noise correlation with the MM AUX-PF with AM and MM AUX-PF with AS. From both Figures 1.13 and 1.14 it is evident that the accuracy of the MM AUX-PF with AS and of the MM-AUX PF with AM is higher than the accuracy of the MM AUX-PF neglecting the temporal noise correlation.

The computational complexity is another important issue that we investigated. The MM AUX-PF execution time increases with the number of maneuvering models used in the implementation. The ratio between the computational time of the MM AUX-PF with 5 models and the computational time of the conventional AUX-PF is approximately 3:1. In the framework of the MATLAB environment, one-step processing time of a mobile node is approximately 2 seconds on a conventional PC (AMD Athlon(tm) 64 Processor 1.81 GHz). By using C++ programming tools the computational time is reduced to the sampling interval. In MATLAB environment with a non-optimised code, the execution time for the MM-AUX PF with AS and AM is 2.33 s and 2.38 s, respectively.

1.8 Conclusions

This chapter presents sequential Monte Carlo methods for solving the problem of simultaneous localisation of mobile nodes in wireless networks with correlated in time measurement noises. The current state-of-the-art is surveyed and then techniques are presented for localisation of multiple mobile nodes, with estimation of

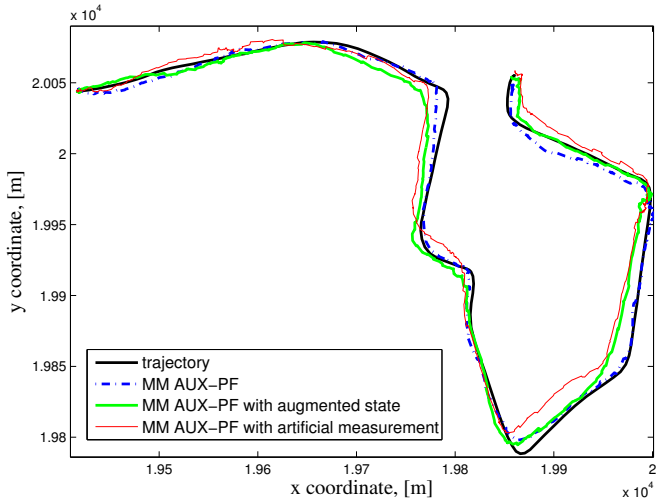

Fig. 1.13. This Figure shows the actual and the estimated trajectory of the vehicle by: *i*) the MM AUX-PF neglecting the measurement noise correlation; *ii*) the MM AUX-PF with augmented state; *iii*) the MM AUX-PF with artificial measurement.

the measurement noise parameters based on received signal strengths. Two multiple model auxiliary particle filters (with an augmented state vector and with an artificial measurement, respectively) are proposed for simultaneous localisation of a mobile nodes in wireless networks. The algorithms performance has been investigated and validated over different scenarios and it has shown high accuracy for localising manoeuvering nodes.

The developed techniques have the potential to be further extended, with other techniques for noise parameter estimation, and their performance studied from theoretical point of view. The developed techniques can also be used in different applications, such as GPS-free position localisation of mobile nodes in wireless networks, for localisation of moving vehicles and robots and combined with different data. The algorithms proposed here can be useful also in scenarios where the location information for the mobile nodes is supporting basic network functions.

Future work will be focused on localisation when both fixed and mobile nodes communicate with each other, on techniques for localising of a large number of nodes, fingerprinting and connectivity issues.

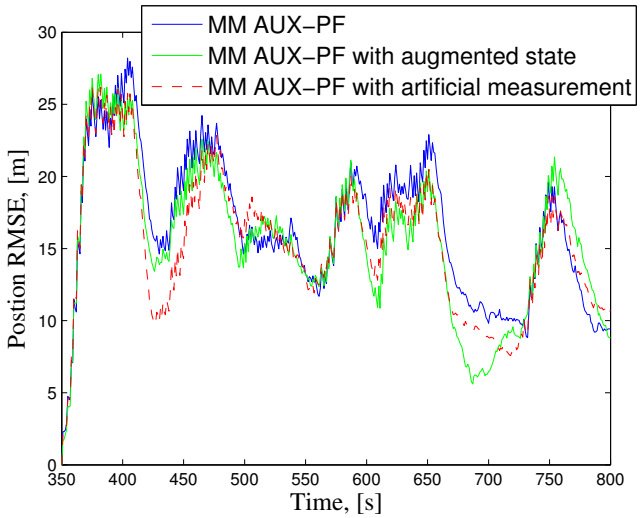

Fig. 1.14. Position RMSE for the: *i*) the MM AUX-PF neglecting the measurement noise correlation; *ii*) the MM AUX-PF with augmented state; *iii*) the MM AUX-PF with artificial measurement.

1.9 Acknowledgements

We acknowledge the support of the [European Community's] Seventh Framework Programme [FP7/2007-2013] under grant agreement No 238710 (Monte Carlo based Innovative Management and Processing for an Unrivalled Leap in Sensor Exploitation), network activities from the EU COST action TU0702 and the Bulgarian National Science Fund, grant DTK02-28/2009. We are grateful also HW Communications, Ltd., UK for providing us with the real data.

References

1. P. Juang, H. Oki, Y. Wang, L. S. Peh, and D. Rubinstein, "Energy-efficient computing for wildlife tracking: Design tradeoffs and early experiences with ZebraNet," in *Proc. Conf. Architectural Support for Programming Languages and Operating Systems*, 2002, pp. 96–107.
2. N. Patwari, J. Ash, S. Kyperountas, A. Hero III, R. Moses, and N. Correal, "Locating the nodes: Cooperative localization in wireless sensor networks," *IEEE Signal Processing Magazine*, vol. 22, no. 4, pp. 54 – 69, 2005.
3. M. Çetin, L. Chen, J. Fisher, A. Ihler III, M. Wainwright, and A. Willsky, "Distributed fusion in sensor networks," *IEEE Signal Proc. Magazine*, vol. 23, no. 4, pp. 42– 55, July 2006.
4. F. Zhao, J. Shin, and J. Reich, "Information-driven dynamic sensor collaboration for tracking applications," *IEEE Signal Processing Magazine*, vol. 19, no. 2, pp. 61–72, March 2002.

5. J.J. Xiao, A. Ribeiro, and Z.-Q. Luo, "Distributed compression-estimation using wireless sensor networks," *IEEE Signal Proc. Magazine*, vol. 23, no. 4, pp. 27–41, 2006.
6. M. Mauve, J. Widmer, and H. Hartenstein, "A survey on position-based routing in mobile ad hoc networks," *IEEE Network Magazine*, vol. 15, no. 6, pp. 30–39, Nov. 2001.
7. M. Srivastava, R. Muntz, and M. Potkonjak, "Smart kindergarten: Sensor-based wireless networks for smart developmental problem-solving environments," in *Proc. of the ACM SIGMOBILE 7th Annual International Conf. on Mobile Computing and Networking*, 2005.
8. F. Gustafsson and F. Gunnarsson, "Mobile positioning using wireless networks: Possibilities and fundamental limitations based on available wireless network measurements," *IEEE Signal Processing Magazine*, vol. 22, no. 4, pp. 41 – 53, 2005.
9. R. Moses, D. Krishnamurthy, and R. Patterson, "A self-localization method for wireless sensor networks," *EURASIP Journal on Applied Signal Processing*, , no. 4, pp. 348–358, 2003.
10. F. Gustafsson, "Particle filter theory and practice with positioning applications," *IEEE Transactions on Aerospace and Electronics Systems Magazine Part II: Tutorials*, vol. 25, no. 7, pp. 53–82, 2010.
11. P. Djuric, M. Vemula, M. Bugallo, and J. Miguez, "Non-cooperative localization of binary sensors," in *Proc. of IEEE Statistical Signal Proc. Workshop*. 2005, France.
12. G. Sun, J. Chen, W. Guo, and K. Liu, "Signal processing techniques in network-aided positioning: a survey of state-of-the-art positioning designs," *IEEE Signal Processing Magazine*, vol. 22, no. 4, pp. 12–23, 2005.
13. K. Chintalapudi, A. Dhariwal, R. Govindan, and G. Sukhatme, "Ad-hoc localization using ranging and sectoring," in *Proc. of the IEEE Infocomm*, 2004.
14. F. Gustafsson and F. Gunnarsson, "Localization in sensor networks based on log range observations," in *Proc. of the 10th International Conf. on Information Fusion*, Canada, 2007.
15. J. Jirod and D. Estrin, "Robust range estimation using acoustic and multimodal sensing," in *Proc. of the IEEE International Conf. on Intelligent Robots and Systems*, 2001.
16. T. He, C. Huang, B. M. Blum, J. A. Stankovic, and T. Abdelzaher, "Range-free localization schemes for large scale sensor networks," in *MobiCom '03: Proc. of the 9th Annual International Conf. on Mobile computing and networking*, NY, USA, 2003, pp. 81–95, ACM Press.
17. H. Liu, H. Darabi, P. Banerjee, and J. Liu, "Survey of wireless indoor positioning techniques and systems," *IEEE Transactions on Systems, Man, and Cybernetics - Part C: Applications and Reviews*, vol. 37, no. 6, pp. 1067 – 1080, 2007.
18. P. Vorst, J. Sommer, C. Hoene, P. Schneider, C. Weiss, T. Schairer, W. Rosenstiel, A. Zell, and G. Carl, "Indoor positioning via three different rf technologies," in *Proceedings of the 4th European Workshop on RFID Systems and Technologies (RFID SysTech 2008)*, Freiburg, Germany, June 10-11 2008, number 209 in ITG-Fachbericht, VDE Verlag.
19. K. Pahlavan, F. Akgul, Y. Ye, T. Morgan, F. Alizadeh-Shabodz, M. Heidari, and C. Steger, "Taking positioning indoors. Wi-Fi localization and GNSS," *Inside GNSS*, May 2010.
20. U. M. Bshara, and Orguner, F. Gustafsson, and L. Van Biesen, "Fingerprinting localization in wireless networks based on received-signal-strength measurements: A case study on WiMAX networks," *IEEE Transactions on Vehicular Technology*, vol. 59, no. 1, pp. 283 –294, 2010.
21. C. Takenga, T. Peng, and K. Kyamakya, "Post-processing of fingerprint localization using Kalman filter and map-matching techniques," in *Proc. of the 9th International Conference on Advanced Communication Technology*, 2007, vol. 3, pp. 2029 –2034.
22. P. K. Engee, "The global positioning system: Signals, measurements and performance," *International Journal of Wireless Information Networks*, vol. 1, no. 2, pp. 83–105, 1994.
23. Z. Zaidi and B. Mark, "A mobility tracking model for wireless ad hoc networks," in *Proc. of IEEE WCNC'03*, March 2003, vol. 3, pp. 1790–1795.
24. Z. Zaidi and B. Mark, "Mobility estimation for wireless networks based on an autoregressive model," in *Proc. of the IEEE Globecom*, 2004, pp. 3405–3409.
25. U. Hammes and A. M. Zoubir, "Robust mobile terminal tracking in NLOS environments based on data association," *IEEE Transactions on Signal Processing*, vol. 58, pp. 5872–5882, 2010.

26. C. Morelli, M. Nicoli, V. Rampa, and U. Spagnolini, "Hidden Markov models for radio localization in mixed LOS/NLOS conditions," *IEEE Trans. on Signal Processing*, vol. 55, no. 4, pp. 1525 – 1542, 2007.
27. L. Hu and D. Evans, "Localization for mobile sensor networks," in *Proc. of the Tenth Annual Intl. Conf. on Mobile Computing and Networking*, USA, 2004.
28. L. Mihaylova, D. Angelova, C.N. Canagarajah, and D.R. Bull, "Algorithms for Mobile Nodes Self-Localisation in Wireless Ad Hoc Networks," in *Proc. of the 9th International Conf. on Information Fusion*, Italy, Florence, 2006.
29. J.M. Huerta, J. Vidal, A. Giremus, and J.-Y. Tourneret, "Joint particle filter and UKF position tracking in severe non-line-of-sight situations," *IEEE Journal of Selected Topics in Signal Processing*, vol. 3, no. 5, pp. 874 – 888, 2009.
30. A. Ihler, J. Fisher, R. Moses, and A. Willsky, "Nonparametric belief propagation for sensor networks," *IEEE Journal on Selected Areas in Communications*, vol. 23, no. 4, pp. 809–819, 2005.
31. L. Mihaylova, D. Bull, D. Angelova, and N. Canagarajah, "Mobility tracking in cellular networks with sequential Monte Carlo filters," in *Proc. of the Eight International Conf. on Information Fusion*, 2005.
32. L. Mihaylova, D. Angelova, S. Honary, D.R. Bull, C.N. Canagarajah, and B. Ristic, "Mobility tracking in cellular networks using particle filtering," *IEEE Transactions on Wireless Communications*, vol. 6, no. 10, pp. 3589–3599, 2007.
33. R. Karlsson and N. Bergman, "Auxiliary particle filters for tracking a manoeuvring target," in *Proceedings of the 39th IEEE Conference on Decision and Control*, 2000, pp. 3891–3895.
34. M. S. Arulampalam, B. Ristic, N. Gordon, and T. Mansell, "Bearings-only tracking of manoeuvring targets using particle filters," *EURASIP Journal on Applied Signal Processing*, vol. 2004, no. 1, pp. 2351–2365, 2004.
35. P. M. Djuric, M. Vemula, and M. F. Bugallo, "Target tracking by particle filtering in binary sensor networks," *IEEE Transactions on Signal Processing*, vol. 56, no. 6, pp. 2229–2238, 2008.
36. A. Kannan, G. Mao, and B. Vucetic, "Simulated annealing based wireless sensor network localization with flip ambiguity mitigation," in *IEEE Vehicular Technology Conference Spring (VTC)*, 2006, pp. 1022 – 1026.
37. M. Gudmundson, "Correlation model for shadow fading in mobile radio systems," *Electronics Letters*, vol. 27, no. 23, pp. 2145–2146, 1991.
38. T. Jiang, N. Sidiropoulos, and G. Giannakis, "Kalman filtering for power estimation in mobile communications," *IEEE Transactions on Wireless Communications*, vol. 2, no. 1, pp. 151–161, 2003.
39. I. Forkel, M. Schinnenburg, and M. Ang, "Generation of two-dimensional correlated shadowing for mobile radio network simulation," in *Proceedings of The 7th International Symposium on Wireless Personal Multimedia Communications, WPMC 2004*, Abano Terme (Padova), Italy, Sep 2004, p. 5.
40. L. Mihaylova, D. Angelova, D. R. Bull, and N. Canagarajah, "Localization of mobile nodes in wireless networks with correlated in time measurement noise," *IEEE Transactions on Mobile Computing*, vol. 10, pp. 44–53, 2011.
41. L. Mihaylova and D. Angelova, "Noise parameters estimation with Gibbs sampling for localisation of mobile nodes in wireless networks," in *Proc. of the 13th International Conference on Information Fusion*, Edinburgh, UK, 2010, pp. tu3.5.1–0037, ISIF.
42. Y. Bar-Shalom, X. Rong Li, and T. Kirubarajan, *Estimation with Applications to Tracking and Navigation*, John Wiley and Sons, 2001.
43. T. Camp, J. Boleng, and V. Davies, "A survey of mobility models for ad hoc network research," *Wireless Communications and Mobile Computing*, vol. 2, no. 5, pp. 483–502, Aug. 2002.
44. B. Mark and Z. Zaidi, "Robust mobility tracking for cellular networks," in *Proc. IEEE Intl. Communications Conf.*, May 2002, pp. 445–449.
45. Z. R. Zaidi and B. L. Mark, "Real-time mobility tracking algorithms for cellular networks based on Kalman filtering," *IEEE Transactions on Mobile Computing*, vol. 4, no. 2, pp. 195–208, 2005.

46. R. Moose, "An adaptive state estimator solution to the maneuvering target tracking problem," *IEEE Transactions on Automatic Control*, vol. 20(3), pp. 359–362, June 1975.
47. Y. Bar-Shalom and X.R. Li, *Estimation and Tracking: Principles, Techniques and Software*, Artech House, 1993.
48. X. R. Li and V. Jilkov, "A survey of maneuveuvering target tracking. Part I: Dynamic models," *IEEE Trans. on Aerosp. and Electr. Systems*, vol. 39, no. 4, pp. 1333–1364, 2003.
49. Z. Yang and X. Wang, "Joint mobility tracking and hard handoff in cellular networks via sequential Monte Carlo filtering," in *Proc. of the IEEE Conf. on Computer Communications (Infocom)*, New York, 2002, pp. 968–975.
50. Z. Yang and X. Wang, "Sequential Monte Carlo for mobility management in wireless cellular networks," in *Proc. of the XI European Signal Processing Conf. (EUSIPCO)*, 2002.
51. G.L. Stüber, *Principles of Mobile Communication. 2nd Edition* , Kluwer Academic Publ., 2001.
52. L.P.I. Hissalle and S. Alahakoon, "Estimating signal strengths prior to field trials in wireless local loop networks," in *Proceedings of the International Conference on Industrial and Information Systems, 2007*, Aug. 2007, pp. 409–414.
53. S. Arulampalam, S. Maskell, N. Gordon, and T. Clapp, "A tutorial on particle filters for online nonlinear/non-Gaussian Bayesian tracking," *IEEE Trans. on Signal Proc.*, vol. 50, no. 2, pp. 174–188, 2002.
54. J. Liu and R. Chen, "Sequential Monte Carlo methods for dynamic systems," *Journal of the American Statistical Association*, vol. 93, no. 443, pp. 1032–1044, 1998.
55. E. Wan and R. van der Merwe, *The Unscented Kalman Filter, Ch. 7: Kalman Filtering and Neural Networks. Edited by S. Haykin*, pp. 221–280, Wiley Publishing, September 2001.
56. M. K. Pitt and N. Shephard, "Filtering via simulation: Auxiliary particle filters," *Journal of the American Statistical Association*, vol. 94, no. 446, pp. 590–599, 1999.
57. S. Saha, E. Ozkan, F. Gustafsson, and V. Smidl, "Marginalized particle filters for Bayesian estimation of Gaussian noise parameters," in *Proc. of the 13th International Conf. on Information Fusion*, UK, 2010, ISIF.
58. E. Ozkan, S. Saha, F. Gustafsson, and V. Smidl, "Non-parametric bayesian measurement noise density estimation in non-linear filtering," in *Proc. of the 36th International Conference on Acoustics, Speech and Signal Processing (ICASSP)*, Prague, Czech Republic, 2011, IEEE.
59. J. H. Kotecha and P. M. Djurić, "Gaussian sum particle filtering," *IEEE Transactions on Signal Processing*, vol. 51, no. 10, pp. 2602–2612, Oct. 2003.
60. S. Geman and D. Geman, "Stochastic relaxation, Gibbs distributions, and the Bayesian restoration of images," pp. 611–634, 1988.
61. J. Diebolt and C. Robert, "Estimation of finite mixture distributions through Bayesian sampling," *J. Royal Stat. Society B*, vol. 56, no. 4, pp. 363–375, 1994.
62. J. Cornebise, M. Maumy, and P. Girard, "A practical implementation of the Gibbs sampler for mixture of distributions: Application to the determination of specifications in food industry," in *Proc. of International Symposium on Applied Stochastic Models and Data Analysis (ASMDA), J. Janssen and P. Lenca (eds)*, 2005, pp. 828–837.